Anharmonic magnetic deformation of self-assembled molecular nanocapsules

O.V. Manyuhina[1], I.O. Shklyarevskiy,[1,2] P. Jonkheijm,[2] P.C.M. Christianen,[1] A. Fasolino,[1] M.I. Katsnelson,[1] A.P.H.J. Schenning,[2] E.W. Meijer,[2] O. Henze,[3] A.F.M. Kilbinger,[3] W.J. Feast,[2,3] and J.C. Maan[1]

[1] Institute for Molecules and Materials, Radboud University Nijmegen,
Toernooiveld 7, 6525 ED Nijmegen, The Netherlands
[2] Laboratory of Macromolecular and Organic Chemistry, Eindhoven University of Technology,
P.O. Box 513, 5600 MB Eindhoven, The Netherlands   and
[3] Department of Chemistry, University of Durham, Durham DH1 3LE, U.K.
(Dated: February 6, 2008)

High magnetic fields were used to deform spherical nanocapsules, self-assembled from bola-amphiphilic sexithiophene molecules. At low fields the deformation – measured through linear birefringence – scales quadratically with the capsule radius and with the magnetic field strength. These data confirm a long standing theoretical prediction (W. Helfrich, Phys. Lett. **43A**, 409 (1973)), and permits the determination of the bending rigidity of the capsules as $(2.6\pm0.8)\times10^{-21}$ J. At high fields, an enhanced rigidity is found which cannot be explained within the Helfrich model. We propose a complete form of the free energy functional that accounts for this behaviour, and allows discussion of the formation and stability of nanocapsules in solution.

The spontaneous formation of hollow molecular spheres (vesicles) is a prototype of self-assembly of organic molecules into well-defined architectures. Vesicular self-assembly is a quite general phenomenon [1] observed in lipid molecules (the building blocks of cell membranes [2]), polymers, dendrimers, and π-conjugated oligomers [3]. This large variety makes vesicles interesting for applications like tailor-made nanocapsules for drug delivery [1], opto-electronics [4], and containers for chemical reactions [5]. They also provide ideal systems to develop physical models for self assembly. Such a model requires a quantitative understanding of the weak non-covalent interactions involved in the self-assembly process on the basis of which vesicle formation and stability can be explained. To this end, we have measured magnetic deformation of novel bola-amphiphilic [6] sexithiophene-based capsules [7, 8] and we have developed a theory to describe this effect. Comparison between theory and experiments allows the determination of important quantities like the bending rigidity of the capsules and contribute to an understanding of their stability.

The determination of the elasticity of vesicles through magnetic deformation was proposed three decades ago by Helfrich [9, 10], but it was never demonstrated experimentally. A magnetic field is a thermodynamic parameter that exerts well-defined magnetic forces to deform all capsules in solution, in a controlled and contact-free way. Furthermore, the field-induced deformation can be quantified via a linear birefringence measurement. The results are, therefore, easier to compare with theory than those of other deformation methods, such as using capillary forces [11, 12, 13], pressure [14, 15], electric fields [16, 17], mechanical forces by an atomic force microscope tip [18] or optical tweezers [19].

Theoretically we use a fourth order Landau-Ginzburg expression of the capsule free energy that describes quantitatively the measured elastic deformation up to high magnetic fields, far beyond the quadratic dependence predicted by Helfrich at low fields [10]. From the data we obtain the free energy as a function of temperature that explains the overall stability of nanocapsules and predicts their dissolution at high temperature. The quantitative determination of the free energy can be used to develop and validate models for the non-covalent interactions responsible for the self-assembly process.

Experimentally we investigate sexithiophene (6T) (2,5'''''-(R-2-methyl-3,6,9,12,15-pentaoxahexadecyl ester), Fig. 1a) which is a π-conjugated oligomer with a rigid apolar sexithiophene block substituted at both ends by polar ethylene oxide chains. 6T forms hollow spherical self-assemblies in a 2-propanol solution (Fig. 1b, details can be found in [8]). Dynamic light scattering (DLS) reveals a narrow distribution of capsule sizes, with an average radius $R(T)$ ($\pm10\%$) that increases with temperature T from 56 nm at 20 °C to 126 nm at 60 °C (Table I). At 70 °C the spherical shape is lost, while at 80°C the scattering intensity is zero because the 6T molecules are molecularly dissolved [8].

6T molecules have a strongly anisotropic diamagnetic susceptibility χ, which means that the sexithiophene core tends to orient along the field [20]. Consequently, capsules are deformed from a sphere to an oblate ellipsoid, where more molecules are parallel (top and bottom of the capsule) than perpendicular to the field (around the equator, Fig. 1c), reducing the magnetic energy at the expense of elastic energy. This magnetic deformation is probed by measuring the field induced optical birefringence Δn in a resistive 20 T magnet using a laser (HeNe, 632.85 nm) modulation technique.

Fig. 1d shows Δn of a 1 g/l 6T/2-propanol solution at different T. These curves were recorded during slow sweeps of the magnetic field B at constant T (±0.1 °C) and are fully reproducible for up-, down-, and consecutive sweeps. In our set-up a negative Δn corresponds to
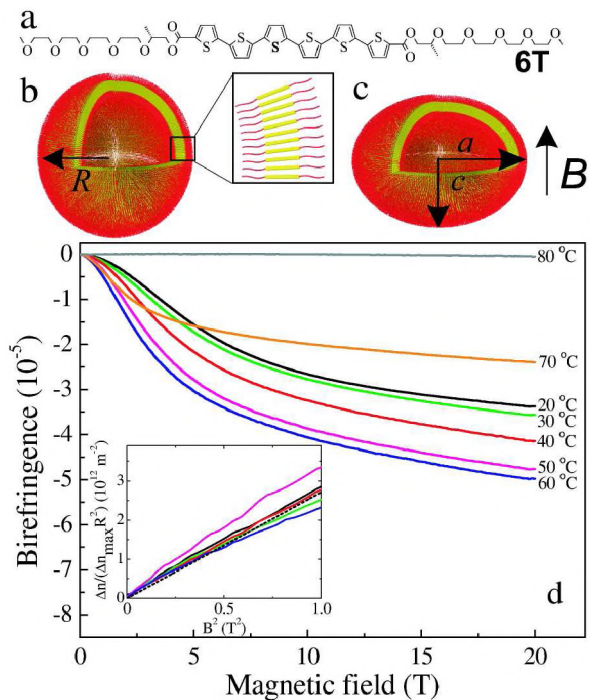

FIG. 1: (color online) a) Chemical structure of a sexithiophene molecule (6T). Schematic representation of a spherical capsule with radius R (b) and magnetically deformed capsule with semi-axes a and c (c) d) Temperature dependence of the magnetic field (B) induced birefringence of a 1 g/l 6T solution in 2-propanol. Inset: normalized birefringence Eq.(3) divided by R^2 and plotted versus B^2. The dashed line corresponds to a fit with constant bending rigidity k.

6T molecules aligning with their long axis parallel to the magnetic field direction, as expected for an oblate ellipsoid (Fig. 1c). The absolute value of Δn increases with T up to 60 °C. At 70 °C it is considerably reduced with a different field dependence, and Δn is zero at 80 °C, when the capsules are dissolved. At low fields Δn scales with the square of the capsule radius and increases as B^2 with approximately the same slope at all temperatures (inset of Fig. 1d). These experimental facts prove that Δn originates from a reversible effect on stable nanocapsules below their melting temperature (20 °C÷60 °C).

For small deformations (low fields) the normalized birefringence $\Delta n/\Delta n_{\max}$ ($\Delta n_{\max} = -6.5 \cdot 10^{-5}$ [21]) varies linearly with deformation [9, 10, 22], but a more accurate relation is needed for high deformations (high fields). For small capsule concentrations ρ_c the refractive index n is related to the polarizability of individual capsules α by $n^2 = n_0^2 + 4\pi\rho_c\alpha$, where n_0 is the refractive index of the solvent. The dipole moment of the 6T molecules $\mathbf{p}$ is connected with the effective electric field $\mathbf{E}'$ in the molecular layer by $\mathbf{p} = \alpha_\perp \left(\mathbf{E}'-\mathbf{e}\left(\mathbf{e}\mathbf{E}'\right)\right)+\alpha_\parallel \mathbf{e}\left(\mathbf{e}\mathbf{E}'\right)$, where $\alpha_\perp$ and $\alpha_\parallel$ are the polarizabilities of 6T molecules with respect to $\mathbf{e}$, the unit vector normal to the capsule at a given point of its surface. Applying standard boundary conditions on the Maxwell equations we find the birefringence of a uniaxially deformed capsule:

$$\Delta n = \pi\rho_c\rho_m \left(\alpha_\parallel \frac{\epsilon_0}{\epsilon_n} - \alpha_\perp\right) \int dS \left(1 - 3e_z^2\right), \quad (1)$$

where ϵ_0 and ϵ_n are the dielectric constants of the solvent and of the 6T in the direction along $\mathbf{e}$, respectively, ρ_m is the surface density of molecules in the layer, the integration is over the surface S of the capsule and z labels the direction of magnetic field $\mathbf{B}$.

To calculate Δn we assume that the shape of the deformed capsules can be described by superspheroids, parameterized by :

$$\begin{aligned}
x(u,v) &= a \cdot \sin^l v \cos u, \\
y(u,v) &= a \cdot \sin^l v \sin u, \\
z(u,v) &= c \cdot \cos^l v, \qquad (a > c),
\end{aligned} \quad (2)$$

with a is the radius in the circular xy plane and c the extension in the z direction (Fig. 1c). Superspheroids are more general than the spheroids ($l = 1$) that are commonly used for small deformations [9, 10], and allow the capsules to flatten ($l < 1$). The birefringence now reads:

$$\frac{\Delta n}{\Delta n_{\max}} = -\frac{1}{2\pi a^2} \int dS \left(1 - 3e_z^2\right). \quad (3)$$

The inset of Fig. 2 shows $\Delta n/\Delta n_{\max}$ as function of deformation $(a - c)/R$ for (super)spheroids. We keep the surface area of the capsule constant, assuming a constant number of 6T molecules that form a permeable membrane. Remarkably, both curves are rather similar, in particular in the low deformation limit, where we recover the linear relationship between Δn and deformation by expanding Eq. (3) as [9, 10, 22]:

$$\frac{\Delta n}{\Delta n_{\max}} \simeq \frac{a - c}{R}, \quad (4)$$

which holds as long as $(a - c)/R \le 0.3$ (inset Fig. 2).

We determine the equilibrium values of a, c and l at each B by minimizing the total free energy $\mathcal{F}_{\text{tot}}$, which is the sum of the elastic $\mathcal{F}_{\text{el}}$ and magnetic $\mathcal{F}_{\text{mag}}$ free energy. Simultaneously, the parameters in $\mathcal{F}_{\text{el}}$ are determined by a fit to the experimental Δn using relation (3). We first consider the well known form of the elastic term proposed by Helfrich [10], leading to:

$$\mathcal{F}_{\text{tot}} = \mathcal{F}_{\text{el}} + \mathcal{F}_{\text{mag}} + \mathcal{F}_{\text{surf}} = \frac{k}{2} \int dS \, H^2 -$$
$$-\frac{\Delta\chi DB^2}{2\mu_0} \int dS \left(e_z^2 - \frac{1}{3}\right) + \gamma \left(\int dS - 4\pi R^2\right)^2, \quad (5)$$

where $H = (\kappa_1 + \kappa_2)/2$ is the mean curvature, κ_1, κ_2 are the principal curvatures, $D = 6.4$ nm (length of long axis of 6T) is the membrane thickness, and $\Delta\chi = \chi_\perp - \chi_\parallel$, the difference in magnetic susceptibility along the short and long axes of 6T respectively [23]. The term $\mathcal{F}_{\text{surf}}$ imposes, for large γ [24], the constraint of constant capsule
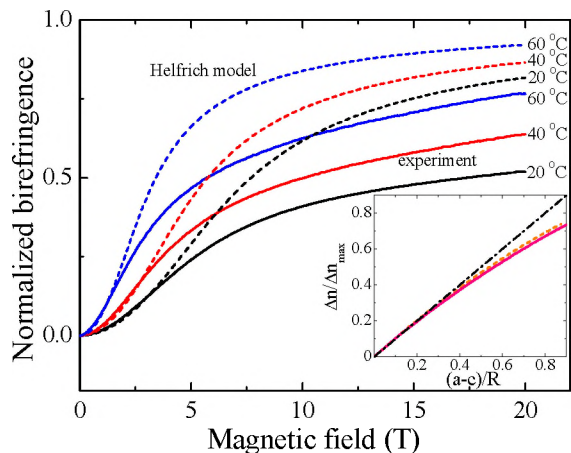
FIG. 2: (color online) Normalized birefringence of magnetically deformed 6T capsules. Solid lines: experimental data for different temperatures. Dashed lines: calculated birefringence in the Helfrich model, fitting the low-field behaviour using a constant k for all T. Inset: calculated relation between birefringence and deformation for superspheroids (solid) and spheroids (dashed) compared to $\Delta n / \Delta n_{\max} \simeq (a - c)/R$ (dash-dotted line).

TABLE I: Structural properties of 6T nanocapsules in 2-propanol at different temperatures. Capsule radius R, as determined by dynamic light scattering (exp.) and obtained by fitting the magnetic birefringence (fit). Equilibrium parameters a, c and l of the deformed capsules at 20 T.

Temperature T ($^\circ C$)	Radius R (nm)		Superspheroid(20 T)		
	Exp.	Fit	a/R	c/R	l
20	56	58	1.19	0.59	0.90
30	68	62	1.20	0.56	0.89
40	75	75	1.23	0.50	0.88
50	88	99	1.26	0.42	0.85
60	126	110	1.28	0.39	0.84

surface. The bending rigidity k is the only fit parameter to obtain the best description of the experimental birefringence (Fig. 2). This approach can be used because the capsule size is large compared to the intermolecular distances, which means that the capsule shape is characterized by its curvatures.

Considering first the limit of small deformations we can expand Eq.(5) as:

$$\frac{a - c}{R} = B^2 \frac{R^2 D \Delta \chi}{3 k \mu_0}. \quad (6)$$

Combination of Eqs. (4) and (6) shows that the low field birefringence is inversely proportional to the bending rigidity k, and scales quadratically with magnetic field and capsule radius (the Helfrich result). Our experimental results (Fig. 2, inset of Fig.1) indeed exhibit this scaling up to $B \sim 1$ T, allowing to determine k as $(2.6 \pm 0.8) \times 10^{-21}$ J, independent of temperature. Our data, therefore, permits the experimental determination of the bending rigidity of this type of capsules.

The Helfrich free energy thus quantitatively describes the birefringence data in the low deformation regime using a constant bending rigidity. However, this model clearly overestimates the experimental birefringence at high fields (Fig. 2), which indicates an increased bending rigidity at higher deformations. Therefore we extend the expression of the free energy by including all symmetry allowed terms up to fourth order [25]:

$$\mathcal{F}_{\mathrm{el}} = \int dS [A'K + AH^2 + c_1 H^4 + c_2 H^2 K + c_3 K^2], \quad (7)$$

where $K = \kappa_1 \kappa_2$ is the Gaussian curvature. Note that terms in HK and H^3 are not allowed for symmetric bola-amphiphiles [25]. Since at $B = 0$ the capsules are spherical, with $H^2 - K = 0$, it is convenient to rewrite $\mathcal{F}_{\mathrm{el}}$ as

$$\mathcal{F}_{\mathrm{el}} = \int dS \big[(A + A')K + A(H^2 - K) + (c_1 + c_2 + c_3)H^4 - \\ - (c_2 + 2c_3)H^2(H^2 - K) + c_3(H^2 - K)^2 \big]. \quad (8)$$

If we compare the elastic energies Eq.(8) for a flat layer and for a set of spheres with radius R with the same total area, and neglecting the edge energy due to the interaction of the solvent with the hydrophobic cores, we find that $A + A' < 0$ and $c_1 + c_2 + c_3 > 0$ must hold to favour the formation of spheres. In this case, the minimum of Eq.(8) occurs for a sphere of radius:

$$R^2 = \frac{1}{H^2} = -2 \frac{c_1 + c_2 + c_3}{A + A'}. \quad (9)$$

Since the term $\int dS A'K$ does not depend on deformation, the magnetic deformation data cannot provide directly information about A'. In fact, according to the Gauss-Bonnet theorem, $\int dS K = 4\pi$ for any surface topologically equivalent to the sphere (like the superspheroid considered here). However, Eq.(9) can be used a posteriori to determine A', once the other parameters are found by a best fit to the experiments. This approach is very powerful, because it experimentally determines the total free energy of nanocapsules, which is very difficult to obtain otherwise, and which can be used to discuss the overall stability of capsules.

Within this description the low field bending constant k can be calculated analytically for spheroids by expanding Eq.(7) for small deformations:

$$k = 2A + \frac{28c_1 + 22c_2 + 16c_3}{3R^2}, \quad (10)$$

which connects our approach to that of Helfrich. Moreover, since k has to be positive to guarantee stability against deformations, this equation poses an extra constraint on the choice of parameters. In the spirit of Landau theory, we assume that only A depends on T and that the coefficients c_i are temperature independent. In fact, by using the experimental value of k we eliminate the parameter A from the fitting procedure, by which c_i
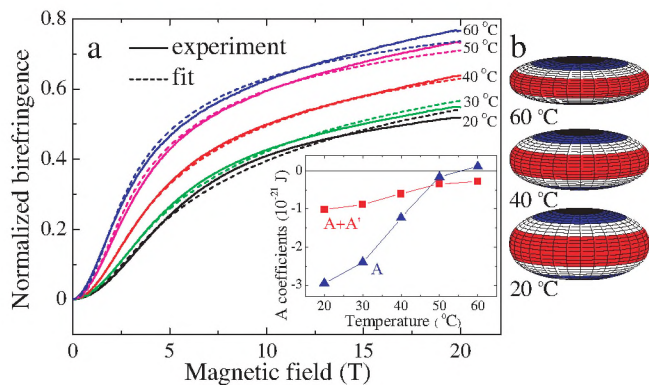
FIG. 3: (color online) a) Fit (dashed lines) of the experimental birefringence (solid lines) at different temperatures, using superspheroidal capsules with deformation energy $\mathcal{F}_{el}$ given by equation (8). b) Equilibrium shapes of the deformed capsules at 20 T.

and $R(T)$ are determined via fitting to the experiments at the different temperatures (Fig. 3a).

For all temperatures the overall behavior of Δn is nicely reproduced, including the weaker field dependence at higher fields, indicating anharmonic deformation characterized by a field enhanced bending rigidity. The fitted value of $R(T)$ (Table I) is well within the error margins of the experimental DLS values. Table I also shows the parameters a, c and l at 20 T, which correspond to substantially deformed capsules, as illustrated in Fig. 3b. At the highest fields deformations $(a - c)/R$ as large as 0.9 are found, which agrees very well with the observed deformation of 6T capsules that are fixed in a compatible organogel and imaged by scanning electron microscopy [8]. Not surprisingly, we find that with increasing deformation the capsule shape becomes flatter (decreasing l, see Table I), maximizing the number of molecules aligned along the field.

The best fits in Fig. 3a are obtained using $c_1 = 1.148, c_2 = -1.336, c_3 = 0.358$ (10^{-35} Jm^2), and the T-dependent A and $A + A'$ are shown in the inset. Indeed, these values make the capsules stable at $B = 0$ ($A + A' < 0, c_1 + c_2 + c_3 > 0$) for $T < 60^\circ C$. However, $A + A'$ approaches 0 when $T \rightarrow 60^\circ C$, suggesting an instability of the capsules at higher T, which is indeed compatible with the experiments that show that the capsules melt above $60^\circ C$. It is this vicinity of the system to an instability, which makes fourth order terms comparable in magnitude to second order ones and make the Helfrich model inadequate for this situation.

The parameters c_1, c_2, c_3, $A(T)$ and $A'(T)$ fully describe the free energy of the nanocapsules. Their actual values are intricately related to the intermolecular interactions within the capsule/solvent system, such as π-π interactions between neighboring 6T cores and interactions between 6T tails and solvent molecules [25, 26]. Determination of these parameters for a physical nanostructure therefore provides a stringent test case, on the basis of which microscopic intermolecular interaction models can be developed. Such a quantitative description of non-covalent interactions within molecular assemblies is an important step towards the detailed understanding of the rules of self-assembly.

[1] M. Antonietti and S. Förster, Adv. Mater. **15**, 1323 (2003).
[2] D.D. Lasic, *Liposomes: ¿From Physics to Applications* (Elsevier, Amsterdam, 1993).
[3] F.J.M. Hoeben *et al.*, Chem. Rev. **105**, 1491 (2005).
[4] T. Piok *et al.*, Adv. Mater. **15**, 800 (2003).
[5] D.M. Vriezema *et al.*, Chem. Rev. **105**, 1445 (2005).
[6] J.-H. Fuhrhop and T. Wang, Chem. Rev. **105**, 2901 (2004).
[7] We use the term capsule instead of vesicle, which is usually used for lipid bilayer systems in aqueous solutions.
[8] I.O. Shklyarevskiy *et al.*, J. Am. Chem. Soc. **127**, 1112 (2005).
[9] W. Helfrich, Z. Naturforsch. **28C**, 693 (1973).
[10] W. Helfrich, Phys. Lett. **43A**, 409 (1973).
[11] D. Needham and E. Evans, Biochemistry **27**, 8261 (1988).
[12] E. Evans and W. Rawicz, Phys. Rev. Lett. **64**, 2094 (1990).
[13] D.V. Zhelev *et al.*, Biophys. J. **67**, 720 (1994).
[14] O.-Y. Zhong-can and W. Helfrich, Phys. Rev. Lett. **59**, 2486 (1987).
[15] P.L.G. Chong *et al.*, Biophys. J. **66**, 2029 (1994).
[16] M. Kummrow and W. Helfrich, Phys. Rev. A **44**, 8356 (1991).
[17] V. Peikov and Z.A. Schelly, J. Phys. Chem. B **105**, 5568 (2001).
[18] Z. Shao and J. Yang, Q. Rev. Biophys. **28**, 195 (1995).
[19] C.-H. Lee *et al.*, Phys. Rev. E **64**, Art. no. 020901 (2001).
[20] G. Maret and K. Dransfeld, in *Strong and Ultra-strong Magnetic Fields and Their Applications* (Springer-Verlag, Berlin, 1985, chap. 4) and ref. therein.
[21] Δn_{max} is the Δn of completely aligned 6T molecules calculated from their anisotropic polarizability: B. Champagne *et al.*, J. Chem. Phys. **100**, 2034 (1994).
[22] G. Maret and K. Dransfeld, Physica **86-88B**, 1077 (1977).
[23] $\chi_{\parallel} = -14.44 \cdot 10^{-6}$, $\chi_{\perp} = -6.45 \cdot 10^{-6}$ D.H. Sutter, W.J. Flygare, J. Am. Chem. Soc. **91**, 4063 (1969).
[24] $\gamma = 225 \cdot 10^9$ J/m^4 in our calculations.
[25] M.I. Katsnelson and A. Fasolino, J. Phys. Chem. B **110**, 30 (2006).
[26] P. Jonkheijm *et al.*, Science **313**, 80 (2006).